ARTICLE

Nanostructure-Mediated Launching and Detection of 2D Surface Plasmons

Jared K. Day,[†,⊥] Oara Neumann,[†,⊥] Nathaniel K. Grady,[†,⊥] and Naomi J. Halas[†,‡,§,⊥,*]

[†]Department of Electrical and Computer Engineering, [‡]Department of Chemistry, [§]Department of Physics, and [⊥]Laboratory for Nanophotonics, Rice Quantum Institute, Rice University, MS-366, 6100 Main Street, Houston, Texas 77005, United States

ABSTRACT Au nanoparticles deposited on a metallic film act as nanoantenna receivers and transmitters for the coupling of free-space radiation into, and out of, 2D surface plasmons. Nanosteps, sub-10-nm gaps between metallic films of differing thickness, can also launch and detect surface plasmons. Here we use both types of structures to locally launch propagating surface plasmon waves and probe their properties. Nanoparticle-launched surface plasmons emerge as two lobes of nominally 90 degree angular width, propagating along the direction of incident polarization. Alternatively, plasmons can be launched unidirectionally, by asymmetric illumination of a nanoparticle receiver.

KEYWORDS: plasmonics · waveguides · surface plasmons · plasmon hybridization · propagation length · nanogap · nanoparticle · metallic film · near-field coupling · transmission · SERS

The ability of small metallic nanoparticles to absorb and scatter electromagnetic energy due to the excitation of their collective electronic resonances (surface plasmons) has motivated the design and fabrication of new plasmonic nanostructures and has given rise to numerous applications. The fact that localized plasmons of metallic nanoparticles much smaller than the wavelength of light can be excited by direct optical illumination has led to their incorporation in solar cells,[1−3] metamaterials,[4] photothermal cancer therapy,[5] and subwavelength waveguiding.[6,7] Optoelectronic device developments have also benefited from the use of surface plasmons on extended structures like metallic films.[8,9] Owing to the momentum mismatch between photons and plasmons, surface plasmons cannot be directly excited on smooth metallic films.[10] Prism-coupling techniques,[10,11] near-field probes or light sources,[9,12,13] fast electron excitation,[14] four-wave mixing,[15] gratings,[16] and individual nanoholes[17] patterned on the surface of metallic films have all been used to excite surface plasmon-polaritons (SPP) in extended structures. In general, these methods may require additional optical devices or fabrication steps. It is therefore highly useful to identify compact, robust methods for exciting and detecting surface plasmons (SPs) with simple far-field optical techniques, which may facilitate the advancement of future plasmon-based devices.

In this article we report the use of two types of nanostructures that can be used for direct excitation of surface plasmons with incident radiation. Individual metallic nanoparticles (NPs) deposited on the surface of metallic films can act as broadband coupling and decoupling agents between photons and surface plasmons (Figure 1). Ensemble measurements have shown that densely populated collections of nanoparticles sitting above metallic films can couple light into surface plasmon modes of the underlying metallic film,[18,19] and individual nanoparticles have been used to couple light both into and out of surface plasmon modes of subwavelength nanowires.[6,20−24] Here we show that plasmonic nanoparticles can act as "receivers", launching surface plasmons by direct optical excitation, and "transmitters", converting surface plasmons into free-space optical waves. Asymmetric nanogaps, or "nanosteps", sub-10-nm discontinuities fabricated into metallic films, can also receive and transmit light, launching and detecting surface plasmons propagating on the metallic film (Figure 1). These structures also allow us to study the excitation characteristics and the propagation properties of surface plasmons launched by these local optical excitation methods. Studying these simple excitation and detection geometries may lead to the development of photon-to-plasmon or plasmon-to-photon nanophotonic components.

*Address correspondence to halas@rice.edu.

Received for review August 11, 2010 and accepted November 9, 2010.

Published online November 19, 2010. 10.1021/nn102003c

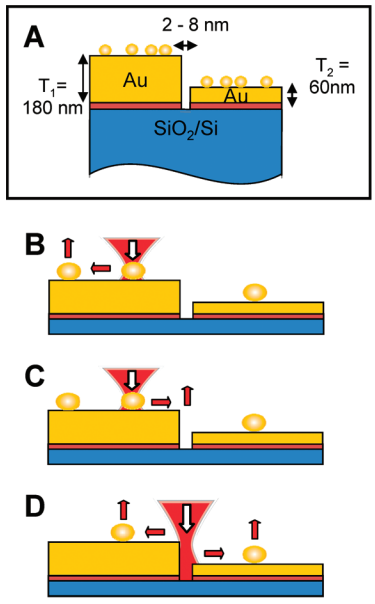

Figure 1. (A) Side view schematic of experimental geometry. Closely spaced metallic slabs attached to a wafer (covered with 200 nm of SiO_2) using a 5 nm thick Ti adhesion layer (red). Individual nanoparticles (NPs) (400−800 nm, not shown to scale) bound to the surface of the slabs are used to excite and detect SPPs. (B) NP-launched SPPs detected *via* NP and (C) *via* "nanostep" junction scattering. (D) Nanostep-launched SPPs detected *via* NP scattering.

STRUCTURE FABRICATION AND ASSEMBLY

Two adjacent Au metallic films of finite (20 − 40 μm) width, separated by a nanostep junction with a width of less than 10 nm, were fabricated using molecular lithography.[25] This method uses a molecular resist consisting of electrostatically assembled self-assembled monolayers (SAMs) interconnected by metal ions to define the separation distance between two smooth metallic films sequentially patterned by photolithography on a Si wafer covered with a 200 nm thick thermal oxide. An initial 5 nm/180 nm thick Ti/Au metallic film was patterned using photolithography and deposited with e-beam evaporation at a rate of 1−2 Å/s. Solution phase deposition was then used to bind monolayers of mercaptohexadecanoic acid, $HS(CH_2)_{15}COOH$, approximately 2 nm thick, on the surface of the first metallic film through the strong attraction of the Au−S bond. Two additional SAMs, were then sequentially attached to the metallic film by alternately depositing a linking species of copper ions (Cu^{2+}) between each SAM[26] to define an approximately 6 nm lift-off mask for subsequent metal deposition. To avoid damaging the protective SAM mask and to obtain more reliable lift-off results, the second Ti/Au film partially overlapped the first film with a reduced thickness ($T_2 \leq T_1/3$) and was deposited at a slower rate (0.5 Å/s). Once the second thinner Ti/Au film, (5 nm/60 nm), was lithographically patterned to overlap the first film, the multilayer SAM mask was chemically removed by immersion in a photoresist stripper, (ACT935, Doe and Ingalls), at 55 °C for approximately 25 min. Better lift-off results were obtained by rinsing the structure in milli-Q water before immersing it in ethanol followed by sonication for 15 s. Nanostep structures were rinsed and dried with milli-Q water, then N_2 gas. This lift-off process leaves behind only the adjacent portion of the second film separated from the first film by a distance equal to the thickness of the multilayer SAM mask.

Au nanoparticles were then randomly dispersed and immobilized on the adjacent metallic films functionalized with poly(4-vinyl pyridine) (PVP) (Sigma-Aldrich).[27,28] The metallic films were functionalized by immersion in a 1% PVP solution in ethanol for 8 h resulting in a PVP adhesion layer approximately 4 nm thick.[29]

These large Au nanoparticles (*ca.* 400−800 nm in diameter) were synthesized according to a simple procedure. A 50 mL aqueous solution of 0.8 M L-ascorbic acid (reagent grade, fine crystal, Fisher Scientific) was directly added under stirring 50 mL aqueous solution of 1% $HAuCl_4$ (Sigma-Aldrich), which was aged for 2−3 weeks under stirring to prevent aggregation. Quickly, a 50 mL diluted PVP solution was then added to coat the newly formed nanoparticles to protect from particle aggregation. This PVP solution was prepared by dissolving 0.354 g in approximately 20 mL of ethanol and diluted with milli-Q water until the final volume reached 50 mL. The solution color turns immediately to a dark red-brown, indicating the formation of well-defined, three-dimensional structures. The Au nanoparticles, coated with a finite amount of PVP, were washed and resuspended in milli-Q water *via* centrifugation.

By depositing Au nanoparticles on the adjacent nanostep-separated metallic films, this structure was capable of supporting several distinct "receiver−transmitter" configurations for exciting and detecting surface plasmons with far-field optics. Figure 1 shows three receiver−transmitter configurations: NP-mediated in-coupling of photons into surface plasmons combined with NP-mediated out-coupling of surface plasmons to photons, NP→NP, (Figure 1B), NP-mediated in-coupling combined with nanostep-mediated out-coupling, NP→nanostep, (Figure 1C), and nanostep-mediated in-coupling combined with NP-mediated out-coupling, nanostep→NP, (Figure 1D). Experimental structures were excited using a diffraction-limited laser spot (either 785 or 980 nm) focused by an inverted optical microscope (Zeiss Axiovert 200 MAT). The polarization of the incident light was controlled using a linear polarizer followed by a half-wave plate. The polarized, collimated laser beam was directed into the microscope using a half-silvered mirror and focused in the image plane using an 100X objective lens (Zeiss, NA = 0.9) in an epi-illumination configuration. The sample was positioned using a piezoelectric stage (Nanonics Imaging, Ltd.). Photons scattered from the sample were detected using a CCD (Axiocam MRm, 1388 × 1040 pixels, spectral range 350−1000 nm).

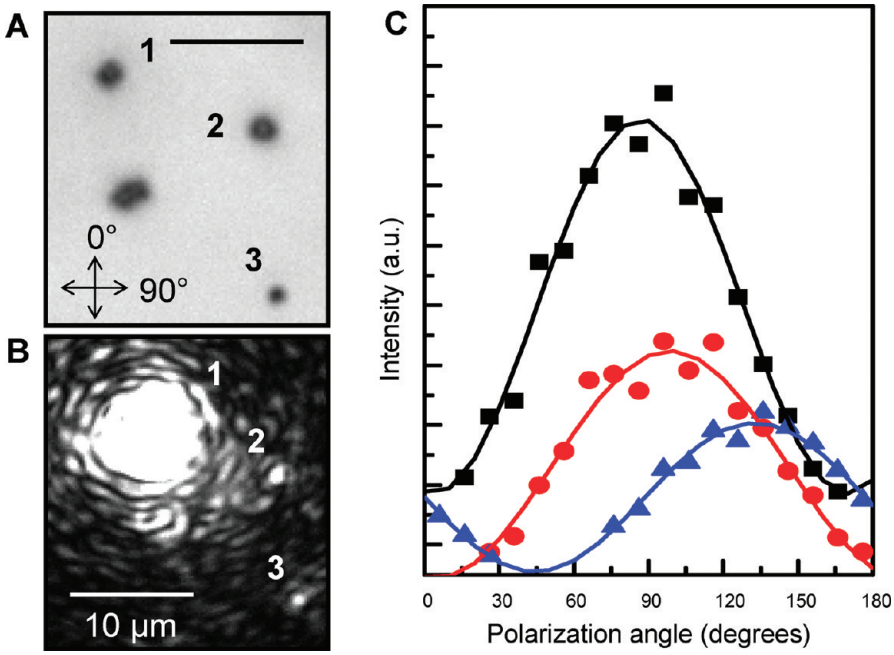

Figure 2. (A) Bright field image of randomly deposited NPs on 180 nm Au film. NP 2 (790 nm diameter) and NP 3 (585 nm diameter) are oriented ~106° and 140° clockwise from NP 1 (400 nm diameter), respectively. (B) Optical image of 785 nm laser incident on NP 1 excites maximum SPP scattering at NPs 2 and 3 for polarization angles of 106° and 140°, respectively. Polarization angle oriented at 130°. (C) Polarization dependent scattering of SPPs: (Black, ■) SPPs excited at NP 1 and scattered at NP 2; 1→2. (Blue, ▲) SPPs excited at NP 1 and scattered at NP 3; 1→3. (Red, ●) SPPs excited at NP 2 and scattered at NP 1; 2→1. Solid lines are best-fit sinusoidal curves.

OPTICAL STUDIES

We first investigate the far-field excitation of surface plasmons through a single NP-film site and the subsequent scattering of surface plasmons back into photons at remote NP-film sites (Figure 2A,B). Despite numerous studies describing the strong electromagnetic interaction of a plasmonic nanoparticle near the surface of a metallic film[19,29−33] little work has been done to analyze the propagation properties of the resulting 2D film plasmon waves that are launched from a NP-film site. A single nanoparticle, (400 nm diameter), resting on a thin layer of PVP attached to an 180 nm thick Au film is used to couple a normal incidence 785 nm laser into the surface plasmons of the underlying film. The nanoparticle breaks the symmetry of the metallic film, allowing the incident light to excite surface plasmons through the nanoparticle induced virtual state.[24,27,28] In essence this coupling results from the Coulomb interaction of the light-induced polarization charge of the nanoparticle and the local surface charges of surface plasmons of the underlying film. This coupling is not a resonant phenomenon and does not require the excitation of a nanoparticle plasmon mode.[24,27,28] The propagation lobes launched from a single NP-film site show a strong polarization dependence, which can be detected by observing the scattered intensity from the nearby nanoparticles. This surface plasmon-scattered intensity is measured from remote nanoparticle sites in Figure 2B. We disregarded light scattering within an extended radius around the laser focus determined by an intensity threshold value to better distinguish nanoparticle scattering from the laser focus. Outside of our threshold-extended laser spot size we identified nanoparticle scattering locations as peak scattering sites that correlated to the physical location of nanoparticle sites, as seen in a corresponding bright-field image (Figure 2A), and contained less than a 5% measurement error (when polarized for maximum scattering intensity) with respect to the background intensity level. Both NP 2 and NP 3 show the highest scattering intensity (Figure 2C) when the polarization angle aligns with the direction of the respective nanoparticle in reference to the excitation site (NP 1). We observe that the NP-mediated coupling of the incident field to plasmons leads to film plasmon propagation that is peaked in the direction of the polarization of the incident light. The azimuthal pattern of the outgoing plasmons is similar to that of a dipole scatterer. This polarization dependence is similar to what has been observed when SPPs are launched from nanohole point sources[34] and when using local illumination from a near-field scanning optical microscope (NSOM) tip.[35,36]

The amplitude of the scattering intensity of the out-coupled light is dependent on nanoparticle size. This is seen in Figure 2C, where we compare the scattering intensities for SPs launched at NP 1 and detected at NP 2 (1→2, black, ■) and the opposite scenario of exciting at NP 2 and measuring at NP 1 (2→1, red, ●). Here we see that the intensity of the scattered light from NP 2 is approximately twice that detected from NP 1. While the far-field scattering cross sections of nanoparticles are well understood,[37] these initial measurements indicate that the far-field to SP and the SP to far-field scattering processes, not unexpectedly, are likely to follow very different scaling laws. It is an interesting observation that in this case the larger far-field signal correlates with the larger nanoparticle "transmitter", not the largest free-space nanoparticle "receiver". Increasing nanoparticle size results in both a redshifting of the nanoparticle-film virtual state and in the increased probability for excitation of higher order nanoparticle modes. Both effects would modify the efficiency of each process and, depending on the frequency of the excitation laser, could result in enhanced surface plasmon-to-free space coupling for the larger nanoparticle.

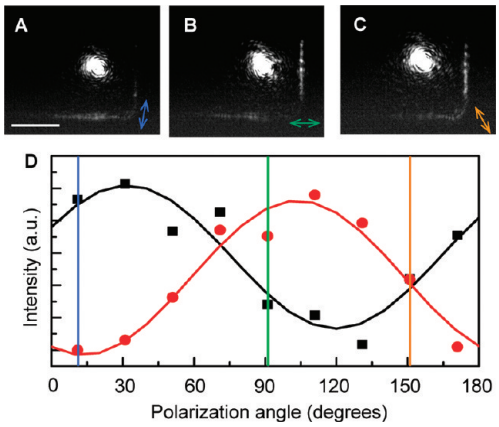

Figure 3. Polarization-dependent scattering of NP-launched surface plasmons from step edges of the Au film. Changes in polarization angle redirect the maximum intensity along nearby uncoupled edges. Panels A, B, and C show the corresponding edge response to 10°, 90°, and 150° polarization orientations, respectively. Scale bar indicates 5 μm. (D) Intensity *versus* polarization angle for scattering at the bottom edge (black, ■) and right edge (red, ●). Solid lines are best-fit sinusoidal curves.

The peak scattering intensity measurements between NPs 1 and 2 are greater than the scattering intensity measured at NP 3 (1→3, blue, ▲) due to the increased distance of NP 3 from the excitation site at NP 1 in comparison with the distance between NP 2 and NP 1.

The directionality of surface plasmon propagation on a metallic film for nanoparticle-mediated in-coupling can also be observed by monitoring the surface plasmon scattering intensity from discontinuities such as the edges of a metallic film. Sharp discontinuities in a metallic film decrease the momentum of the surface plasmons, enabling them to scatter into photons. Figure 3 shows nanoparticle-mediated surface plasmon excitation at a wavelength of 785 nm from a nanoparticle (533 nm in diameter) that results in SPP scattering from two orthogonal edges of a 180 nm thick Au film. As the polarization angle is rotated, the surface plasmon scattering is redirected from the bottom edge to the right edge (Figure 3A−C). Maximum plasmon scattering from either the right or bottom edge should occur when the polarization angle is perpendicular to the edges, directed along the shortest distance to the respective edge. However, due to the small structural variations of the nanoparticle and surface roughness of the underlying film, maximum scattering occurs slightly off the perpendicular axis in this case (Figure 3D). Total edge scattering intensity was obtained by integrating the intensities from a 20-pixel rectangular area, within 40° of the excitation site, in the image surrounding each edge. This shows that nanoparticle-mediated surface plasmon excitation can address extended structures in specific directions controlled by an input polarization angle, a property that could enable the excitation of multiple emitters by surface plasmons in the same directional cone.

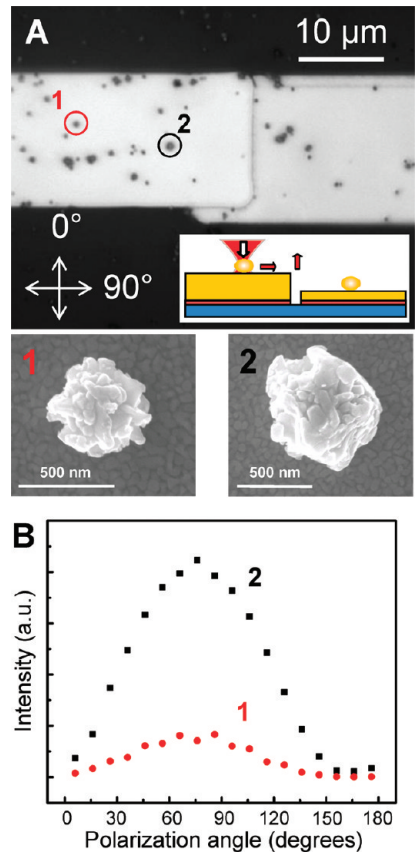

Figure 4. Nanostep scattering of NP-mediated SPPs. (A) Brightfield and SEM images of nanoparticle-decorated stepped film structure. NP 1 and 2 are ~20 and 10 μm from the nanostep junction. (B) Step scattering as a function of polarization angle for both NP→nanostep excitation sites. Peak scattering occurs when the E-field is oriented perpendicular to the nanostep.

Similar to a film edge, a nanostep junction between two adjacent metallic films is also a discontinuity that can serve as a conversion site for surface plasmons into photons (Figure 4). We compare the scattering intensity from a nanostep as a function of polarization angle for nanoparticle in-coupling sites positioned at different distances from the nanostep. The surface plasmons were optically excited through individual nanoparticles labeled as NP 1 (534 nm diameter) and NP 2 (765 nm diameter) on a thick metallic film (180 nm) using a 785 nm laser (Figure 4A). The cumulative scattering from the nanostep was measured as the integrated scattering intensity within a 10 pixel rectangular area around the nanostep (Figure 4B). As for the edge in Figure 3, maximum intensity occurs for polarization perpendicular to the nanostep, confirming that the direction of the surface plasmons launched from a nanoparticle is in the direction of incident polarization. Figure 4B also shows the attenuation of surface plasmons detected at the nanostep when launched from nanoparticles at two different distances from the step (this is discussed in greater detail below).

The asymmetric launching of SPPs from a nanoparticle-mediated coupling site can also occur

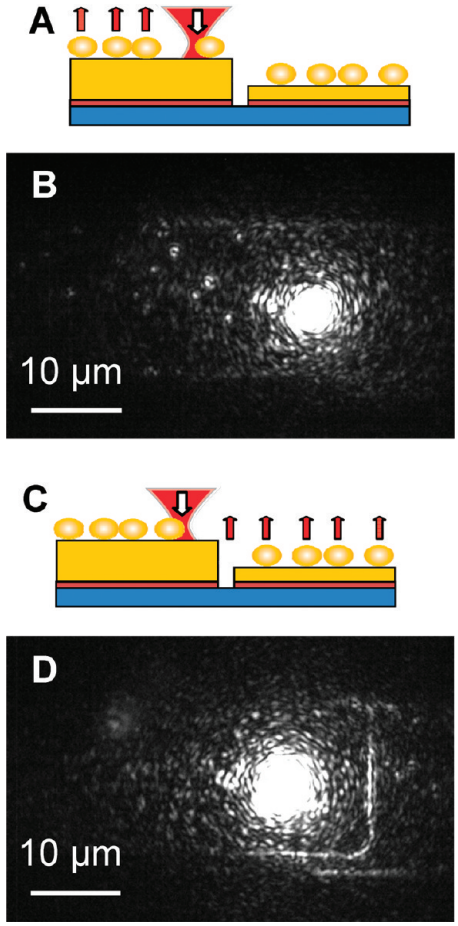

Figure 5. Film plasmons launched asymmetrically from a single NP-film site in two opposite directions. Schematic and optical scattering image of SPPs launched left toward the NPs on the thick film (A, B) and right toward the nanostep junction and the thin film (C, D).

when the laser spot illuminates only a portion of the physical cross section of the nanoparticle (Figure 5). Scattering images show that the same nanoparticle in-coupling site (765 nm diameter) on the thick portion of the two adjacent films (180 nm) can preferentially launch SPPs in two opposing directions. Depending on placement of the laser focusing spot on the nanoparticle, surface plasmons can be launched to the left, toward multiple nanoparticle scatterers on the left portion of the film (Figure 5A,B) or to the right toward the nanostep (Figure 5C,D) for the same polarization angle (90°). This position-dependent coupling of free-space optical waves to propagating surface plasmons causes a 2D surface propagation lobe that is predominately inclined toward the brighter side of the nanoparticle (Figure 5A,C). This directional plasmon excitation is accessible for larger nanoparticles such as those used here (for particle diameters of the same order or greater than the half-wavelength of the excitation laser), where changing the position of the laser spot alters the optical field gradients at the illuminated nanoparticle. This addressability may be important in applications, such as directional plasmon routing controlled by positioning of both the excitation beam and the nanostructure launch site.

Surface plasmons are also transmitted across a sub-10 nm film gap. Directing SPPs toward the nanostep junction allows it to be used as a scattering site for detecting SPPs as shown previously (Figure 4B). In addition SPPs can also "tunnel" across the nanostep junction because of the high near-field coupling between two closely spaced metallic films. The transmission of surface plasmons between metallic films can be verified by the observation of plasmon scattering at multiple nanoparticle sites on the thinner metallic film (60 nm) located to the right of the excitation site on the thick metallic film in Figure 5D. The transmission of SPPs across the nanostep is possible despite the large (3:1) thickness disparity between the two films.

Observing the scattering from multiple NP-film sites, (Figure 6A−C), at different distances from the excitation site enabled us to measure the wavelength-dependent propagation distance, L_{spp}, of the surface plasmons on Au films decorated with randomly positioned nanoparticles. The propagation distance for surface plasmons is defined as the distance where the intensity of the SPP mode falls to $1/e$ of its initial value. The scattered intensity from multiple nanoparticles as a function of distance from excitation sites was measured using nanoparticle-mediated in-coupling (Figure 6A,C) as well as nanostep-mediated in-coupling (Figure 6B). Nanoparticles within a 30° solid angle trajectory away from the excitation site were monitored to determine the propagation length, to minimize contributions to propagation loss due to plasmon scattering from film edges. Scattering measurements for individual nanoparticles were plotted as a function of distance from the center of the laser spot and fit with an exponential $I(r) = I_o \exp(-r/L_{spp})$, to determine L_{spp} for each configuration (Figure 6D−F).

Using a single plasmonic nanostep structure, three different configurations were chosen to measure the intensity of the surface plasmon scattering from remote nanoparticle sites (Figure 6A−C). The nanoparticle in-coupling and nanoparticle out-coupling configuration excited at 785 nm (Figure 6A) used individual nanoparticles as discrete remote scattering sites of surface plasmon energy displaced from a left-partially eclipsed excitation nanoparticle (765 nm in diameter). The nanoparticles to the left of the excitation site were excited by asymmetrically launching plasmons to that side of the structure. The plasmon decay length, L_{spp}, determined from the distance-dependent intensities of six nanoparticle scattering sites, was measured to be 3.5 ± 1.7 μm (Figure 6A). The proximity of the laser focus to the nanoparticles in Figure 6A may have led to an additional contribution to the measured scattering intensity for the particles and, as a systematic source of error, may have contributed to the lower-than expected value of the propagation distance obtained in this analysis. However, SPPs excited at the same wavelength in the

nanostep in-coupling and nanoparticle out-coupling configuration, nanostep→NP, measured a similar propagation length of 3.21 ± 0.67 μm with nanoparticles much further from the laser focus (Figure 6B). The width of the nanostep, being much smaller than the half-wavelength of any laser in the near-infrared spectrum, couples poorly to the 785 nm laser and only excites a strong surface plasmon wave when the laser is off gap center, in the direction of one of the films. Surface plasmon scattering was therefore detectable only from nanoparticle scattering sites on one film at a time. Nanostep-mediated in-coupling was observed to produce a much stronger plasmon wave, as monitored by nanoparticle out-coupling, for the thicker film than for the thinner film.

The experimentally measured propagation distances for all three configurations are measured to be smaller by a factor of approximately 2 when compared with the calculated propagation distance of surface plasmons on a smooth Au film covered with a dielectric layer.[10] The propagation length measured in our structure is dependent not only on film quality and intrinsic damping, but is also affected by additional loss due to in-plane and radiative scattering from the densely populated nanoparticles that allow us to measure the surface plasmon propagation characteristics. The extent to which nanostructure transmitter and receiver structures induce loss in the propagating surface plasmons by virtue of their size and position is a topic for further, systematic study.

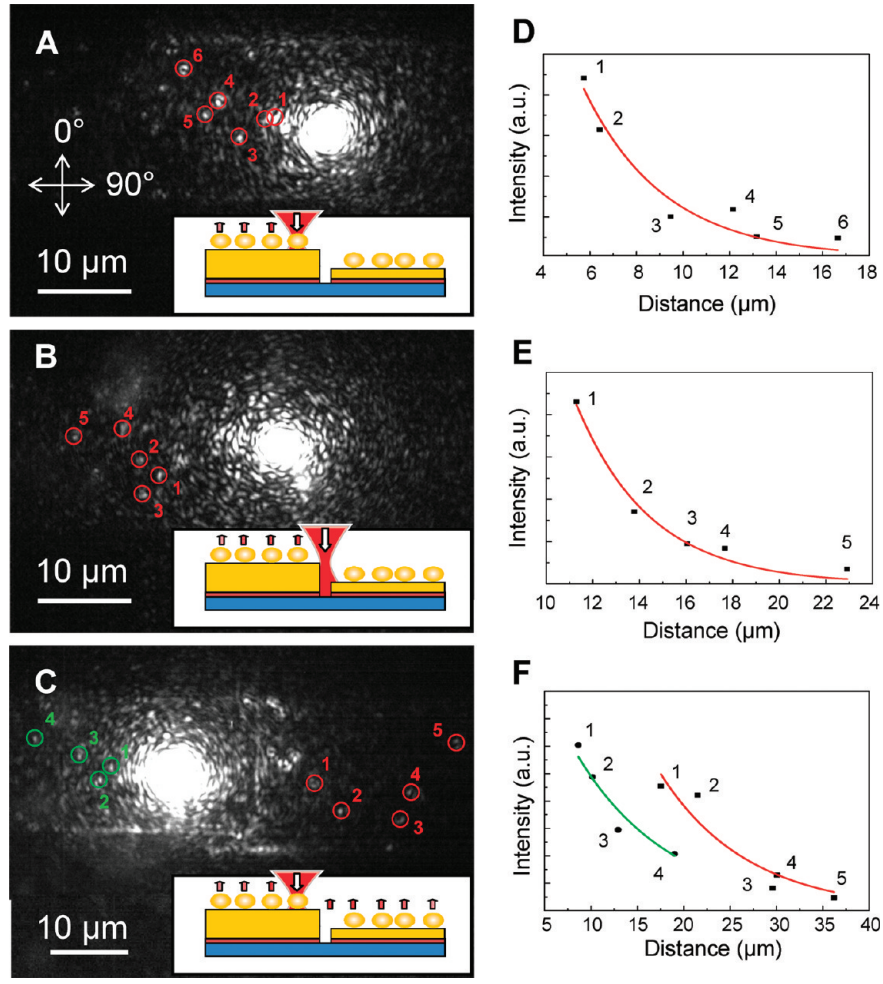

Figure 6. Scattering images for different "receiver→transmitter" configurations (A−C) with corresponding plots of SPP scattering of individual NPs as a function of distance from the laser spot (D−F). Exponential fits are plotted in solid lines. The 785 nm laser excites NP→NP configuration (A, D) and nanostep→NP (B, E). NP→NP configuration excited at 980 nm wavelength (C, F). All images are shown with a polarization angle of 90°. Insets show schematics for each configuration.

Surface plasmon scattering from nanoparticles on both coupled films can more easily be seen at longer wavelengths where Au films are less absorbing (Figure 6C). The transmission of surface plasmons between films of different heights allowed us to measure the propagation length for both films simultaneously using nanoparticle scattering. Utilizing a 980 nm laser to excite the same nanoparticle (765 nm diameter) used in Figure 6A, we determined the values of L_{spp} for both the thick and thin metallic films to be 10.09 ± 3.64 and 9.39 ± 1.23 μm, respectively. The propagation loss is slightly greater for the case where the plasmon is excited on the thicker film and traverses to the thinner film. These measurements may provide a method for quantifying propagation losses at nanosteps or similar types of structures. In this case, the surface plasmon is observed on both the thick and the thin film sides of the nanoparticle (Figure 6C), which is due to the longer plasmon propagation length for this excitation wavelength.

SUMMARY

We have shown that nanoparticle- and nanostep-mediated coupling of free space optical waves into and out of surface modes of a plasmonic film are effective ways to locally excite and interrogate surface plasmons. The NP-film coupling results in a broad virtual state,[29] allowing the nanoparticle to function as a nanoantenna that can both couple free-space radiation into surface plasmon modes and scatter propagating surface plasmons into free-space radiation. Standard approaches for SPP excitation such as prism coupling in a Kretschmann geometry, the use of periodic structures such as gratings and arrays, or the recently reported use of four-wave mixing typically result in unidirectional launching of surface plasmons.[9−16] Unlike these approaches, nanoparticle-based SPP launching is local to the nanoparticle site, easily di-

rected by rotation of the incident light polarization, and can be either unidirectional or bidirectional, depending on the relative position of the laser focus with respect to the nanoparticle antenna. Further development of these types of highly compact nanoparticle-film transmitters and receivers may lead to new methods for the coupling of optical signals to on-chip networks capable of performing logic or computational functions, then transmit the outcome off-chip, back into free space.

Acknowledgment. The authors thank J. Britt Lassiter and Nikolay Mirin for valuable discussions and insights. This work was supported by the NSF IGERT fellowship (J.D.) under Grant No. DGE-0504425, the Welch Foundation under Grant C-1220, and the Department of Defense National Security Science and Engineering Faculty Fellowship (NSSEFF) Grant No. N00244-09-0067.

REFERENCES AND NOTES

1. Atwater, H. A.; Polman, A. Plasmonics for Improved Photovoltaic Devices. *Nat. Mater.* **2010**, *9*, 205–213.
2. Rand, B. P.; Peumans, P.; Forrest, S. R. Long-Range Absorption Enhancement in Organic Tandem Thin-Film Solar Cells Containing Silver Nanoclusters. *J. Appl. Phys.* **2004**, *96*, 7519–7526.
3. Schaadt, D. M.; Feng, B.; Yu, E. T. Enhanced Semiconductor Optical Absorption *via* Surface Plasmon Excitation in Metal Nanoparticles. *Appl. Phys. Lett.* **2005**, *86*, 063106.
4. Mirin, N. A.; Halas, N. J. Light-Bending Nanoparticles. *Nano Lett.* **2009**, *9*, 1255–1259.
5. Gobin, A. M.; Lee, M. H.; Halas, N. J.; James, W. D.; Drezek, R. A.; West, J. L. Near-Infrared Resonant Nanoshells for Combined Optical Imaging and Photothermal Cancer Therapy. *Nano Lett.* **2007**, *7*, 1929–1934.
6. Knight, M. W.; Grady, N. K.; Bardhan, R.; Hao, F.; Nordlander, P.; Halas, N. J. Nanoparticle-Mediated Coupling of Light into a Nanowire. *Nano Lett.* **2007**, *7*, 2346–2350.
7. Sanders, A. W.; Routenberg, D. A.; Wiley, B. J.; Xia, Y. N.; Dufresne, E. R.; Reed, M. A. Observation of Plasmon Propagation, Redirection, and Fan-Out in Silver Nanowires. *Nano Lett.* **2006**, *6*, 1822–1826.
8. Dionne, J. A.; Diest, K.; Sweatlock, L. A.; Atwater, H. A. PlasMOStor: A Metal-Oxide-Si Field Effect Plasmonic Modulator. *Nano Lett.* **2009**, *9*, 897–902.
9. Koller, D. M.; Hohenau, A.; Ditlbacher, H.; Galler, N.; Reil, F.; Aussenegg, F. R.; Leitner, A.; List, E. J. W.; Krenn, J. R. Organic Plasmon-Emitting Diode. *Nat. Photonics* **2008**, *2*, 684–687.
10. Raether, H. *Surface-Plasmons on Smooth and Rough Surfaces and on Gratings*; Springer-Verlag: Berlin, 1988; Vol. 111, pp 1−133.
11. Bouhelier, A.; Huser, T.; Tamaru, H.; Guntherodt, H. J.; Pohl, D. W.; Baida, F. I.; Van Labeke, D. Plasmon Optics of Structured Silver Films. *Phys. Rev. B* **2001**, *6315*, 155404.
12. Dallapiccola, R.; Dubois, C.; Gopinath, A.; Stellacci, F.; Dal Negro, L. Near-Field Excitation and Near-Field Detection of Propagating Surface Plasmon Polaritons on Au Waveguide Structures. *Appl. Phys. Lett.* **2009**, *94*, 243118.
13. Akimov, A. V.; Mukherjee, A.; Yu, C. L.; Chang, D. E.; Zibrov, A. S.; Hemmer, P. R.; Park, H.; Lukin, M. D. Generation of Single Optical Plasmons in Metallic Nanowires Coupled to Quantum Dots. *Nature* **2007**, *450*, 402–406.
14. Bashevoy, M. V.; Jonsson, F.; Krasavin, A. V.; Zheludev, N. I.; Chen, Y.; Stockman, M. I. Generation of Traveling Surface Plasmon Waves by Free-Electron Impact. *Nano Lett.* **2006**, *6*, 1113–1115.
15. Renger, J.; Quidant, R.; van Hulst, N.; Novotny, L. Surface-Enhanced Nonlinear Four-Wave Mixing. *Phys. Rev. Lett.* **2010**, *104*, 046803.
16. Devaux, E.; Ebbesen, T. W.; Weeber, J. C.; Dereux, A. Launching and Decoupling Surface Plasmons *via* Micrograting. *Appl. Phys. Lett.* **2003**, *83*, 4936–4938.
17. Yin, L. L.; Vlasko-Vlasov, V. K.; Pearson, J.; Hiller, J. M.; Hua, J.; Welp, U.; Brown, D. E.; Kimball, C. W. Subwavelength focusing and guiding of surface plasmons. *Nano Lett.* **2005**, *5*, 1399–1402.
18. Lal, S.; Westcott, S. L.; Taylor, R. N.; Jackson, J. B.; Nordlander, P.; Halas, N. J. Light Interaction between Gold Nanoshells Plasmon Resonance and Planar Optical Waveguides. *J. Phys. Chem. B* **2002**, *106*, 5609–5612.
19. Hayashi, S.; Kume, T.; Amano, T.; Yamamoto, K. A New Method of Surface Plasmon Excitation Mediated by Metallic Nanoparticles. *Jpn. J. Appl. Phys.* **1996**, *35*, L331–L334.
20. Hao, F.; Nordlander, P. Plasmonic Coupling between a Metallic Nanosphere and a Thin Metallic Wire. *Appl. Phys. Lett.* **2006**, *89*, 103101.
21. Fang, Y. R.; Wei, H.; Hao, F.; Nordlander, P.; Xu, H. X. Remote-Excitation Surface-Enhanced Raman Scattering Using Propagating Ag Nanowire Plasmons. *Nano Lett.* **2009**, *9*, 2049–2053.
22. Hutchison, J. A.; Centeno, S. P.; Odaka, H.; Fukumura, H.; Hofkens, J.; Uji-i, H. Subdiffraction Limited, Remote Excitation of Surface Enhanced Raman Scattering. *Nano Lett.* **2009**, *9*, 995–1001.
23. Felidj, N.; Aubard, J.; Levi, G.; Krenn, J. R.; Schider, G.; Leitner, A.; Aussenegg, F. R. Enhanced Substrate-Induced Coupling in Two-Dimensional Gold Nanoparticle Arrays. *Phys. Rev. B* **2002**, *66*, 245407.
24. Wei, H.; Hao, F.; Huang, Y. Z.; Wang, W. Z.; Nordlander, P.; Xu, H. X. Polarization Dependence of Surface-Enhanced Raman Scattering in Gold Nanoparticle−Nanowire Systems. *Nano Lett.* **2008**, *8*, 2497–2502.
25. Hatzor, A.; Weiss, P. S. Molecular Rulers for Scaling Down Nanostructures. *Science* **2001**, *291*, 1019–1020.
26. Anderson, M. E.; Tan, L. P.; Tanaka, H.; Mihok, M.; Lee, H.; Horn, M. W.; Weiss, P. S. Advances in Nanolithography Using Molecular Rulers. *J. Vac. Sci. Technol., B* **2003**, *21*, 3116–3119.
27. Malynych, S.; Luzinov, I.; Chumanov, G. Poly(vinyl pyridine) as a Universal Surface Modifier for Immobilization of Nanoparticles. *J. Phys. Chem. B* **2002**, *106*, 1280–1285.
28. Le, F.; Lwin, N. Z.; Halas, N. J.; Nordlander, P. Plasmonic Interactions between a Metallic Nanoshell and a Thin Metallic Film. *Phys. Rev. B* **2007**, *76*, 165410.
29. Le, F.; Lwin, N. Z.; Steele, J. M.; Kall, M.; Halas, N. J.; Nordlander, P. Plasmons in the Metallic Nanoparticle−Film System as a Tunable Impurity Problem. *Nano Lett.* **2005**, *5*, 2009–2013.
30. Hu, M.; Ghoshal, A.; Marquez, M.; Kik, P. G. Single Particle Spectroscopy Study of Metal-Film-Induced Tuning of Silver Nanoparticle Plasmon Resonances. *J. Phys. Chem. C* **2010**, *114*, 7509–7514.
31. Mock, J. J.; Hill, R. T.; Degiron, A.; Zauscher, S.; Chilkoti, A.; Smith, D. R. Distance-Dependent Plasmon Resonant Coupling between a Gold Nanoparticle and Gold Film. *Nano Lett.* **2008**, *8*, 2245–2252.
32. Ruppin, R. Surface-Modes and Optical-Absorption of a Small Sphere Above a Substrate. *Surf. Sci.* **1983**, *127*, 108–118.
33. Takemori, T.; Inoue, M.; Ohtaka, K. Optical-Response of a Sphere Coupled to a Metal-Substrate. *J. Phys. Soc. Jpn.* **1987**, *56*, 1587–1602.
34. Yin, L.; Vlasko-Vlasov, V. K.; Rydh, A.; Pearson, J.; Welp, U.; Chang, S. H.; Gray, S. K.; Schatz, G. C.; Brown, D. B.; Kimball, C. W. Surface Plasmons at Single Nanoholes in Au Films. *Appl. Phys. Lett.* **2004**, *85*, 467–469.
35. Sonnichsen, C.; Duch, A. C.; Steininger, G.; Koch, M.; von Plessen, G.; Feldmann, J. Launching Surface Plasmons into Nanoholes in Metal Films. *Appl. Phys. Lett.* **2000**, *76*, 140–142.
36. Baida, F. I.; Van Labeke, D.; Bouhelier, A.; Huser, T.; Pohl, D. W. Propagation and Diffraction of Locally Excited Surface Plasmons. *J. Opt. Soc. Am. A* **2001**, *18*, 1552–1561.
37. Bohren, C. F.; Huffman, D. R. *Absorption and Scattering of Light by Small Particles*; Wiley: New York, 1983; p xiv, 530 p.